JVSTB
JOURNAL OF VACUUM SCIENCE AND TECHNOLOGY B

Bond contribution model for the prediction of glass transition temperature in polyphenol molecular glass resists

Richard A. Lawson, Wei-Ming Yeh, and Clifford L. Henderson

Citation: J. Vac. Sci. Technol. B **27**, 3004 (2009); doi: 10.1116/1.3250264
View online: http://dx.doi.org/10.1116/1.3250264
View Table of Contents: http://avspublications.org/resource/1/JVTBD9/v27/i6
Published by the AVS: Science & Technology of Materials, Interfaces, and Processing

Bond contribution model for the prediction of glass transition temperature in polyphenol molecular glass resists

Richard A. Lawson, Wei-Ming Yeh, and Clifford L. Henderson[a)]
School of Chemical and Biomolecular Engineering, Georgia Institute of Technology, Atlanta, Georgia 30332-0100

(Received 24 July 2009; accepted 21 September 2009; published 4 December 2009)

Molecular glass resists have shown potential as replacements for polymeric resists in next generation lithography, especially extreme ultraviolet lithography. One of the main concerns about molecular resists is their glass transition temperature (T_g) which can be very low in some cases due to their small molecular size and other factors. While most of the polymeric chemically amplified resist platforms used thus far have T_g's above 100 °C, molecular resists investigated in the literature so far have shown a wide range of measured T_g's from near room temperature to greater than 160 °C. This potential for low T_g values and the current lack of ability to easily predict their T_g is a concern when designing new compounds because a molecular resist may be synthesized with a T_g value that is too low for the required processing conditions (e.g., allowing for dewetting of the resist, flow of the resist features, or excessive photoacid diffusion). To enable rational molecular resist design and overcome these problems, a quantitative structure-property relation model based on bond additivity that allows for the prediction of the T_g of molecular resists based on their full chemical structure has been developed in this work. The model shows a good coefficient of determination (R^2) of 0.84 with experimental data, and a standard deviation of only 12 °C for 57 compounds. It works well across multiple different levels of protection, different structural moieties, different molecular sizes, and different types of protecting groups. The model was also simplified to provide a simple heuristic for predicting T_g based on only two or three structural parameters, and this easy to use simplified model provides a similar level of quantitative agreement with experimental data to the full bond additivity model. © *2009 American Vacuum Society.* [DOI: 10.1116/1.3250264]

I. INTRODUCTION

Molecular glasses are low molecular weight organic compounds that readily form stable amorphous glasses and show many properties associated with polymers including exhibition of a glass transition temperature.[1] Molecular glass photoresists, which are also referred to as molecular resists, have received much attention as potential replacements for polymers in photoresists due to several potential advantages. They were originally introduced because it was thought that the effective reduction in resist molecule pixel size would improve line edge roughness (LER).[2–4] Their small molecule nature also provides additional advantages such as the fact that their synthesis and purification can be precisely controlled to create monodisperse resists with well-defined structure and properties. This precise molecular synthesis control is in contrast with polymeric resists which generally have a polydispersity in molecular weight, chain composition, and monomer order along the chain. This variation in polymer structure leads to physiochemical inhomogeneities in the resist that translates into variations in the dissolution behavior and imaging performance in the resist. The working hypothesis that motivates much of this work is that reducing such compositional inhomogeneities will lead to optimal lithographic performance in resist materials. This concept has been validated to some degree since reduction in the inhomogeneity and polydispersity in molecular resists has already been shown to improve LER.[5–7] A yet untapped but potentially very important property of molecular resists is that the well defined molecular structure of molecular resists offers the ability to develop accurate predictive structure-property models for a variety of important lithographic properties such as glass transition temperature (T_g) and development rate. Many such predictive models for organic compounds have already been developed for nonlithographic properties such as boiling point,[8,9] vapor pressure,[10,11] critical temperature and pressure,[12] flash point,[13] and a number of other parameters.[14] The goal of the work presented here was to develop such a predictive model for the glass transition temperature of molecular resists that could be used to guide their rational design with T_g values in desired ranges.

Despite the advantages of molecular resists, the concept of using molecular resists for high volume manufacturing as replacements for polymeric resists has met some resistance. One commonly cited issue that has led to this resistance is again the concern about their T_g's being lower than that of the polymers conventionally used as photoresists. It is desired that the postapply bake temperature of a photoresist be slightly above its T_g in order to remove a large amount of the residual casting solvent and to minimize the free volume in the film,[15] but it is also desired that the postexposure bake (PEB) temperature be below or only slightly above its T_g to reduce photoacid diffusion during the PEB.[16] For most of the polymer resists used in manufacturing, their T_g is in the

a)Author to whom correspondence should be addressed; electronic mail: cliff.henderson@chbe.gatech.edu

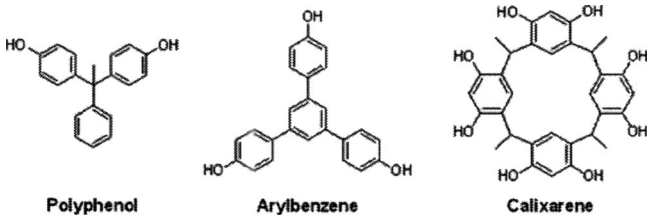

FIG. 1. Representative chemical structures of some of the different families of molecular resists.

range 110–150 °C. This relatively high T_g was particularly important in early chemically amplified resists that required PEB temperatures above approximately 110 °C to catalyze the deprotection reaction responsible for the solubility switch in the materials. Many early reported molecular resists exhibited T_g values below 100 °C.[17] This could be an important issue if the T_g in the molecular resist is so low that at the temperatures required for deprotection (i.e., in positive tone systems) or cross-linking (i.e., negative tone systems) that the PEB would be significantly above the film T_g. Baking too far above the resist T_g has a strong and generally negative effect on many lithographic properties including resolution and line edge roughness due to the fact that diffusion in the film (e.g., photoacid diffusion) is greatly enhanced as the film temperature increases above the film T_g.[18,19] Higher diffusion of photoacid in the resist leads to pattern blur and ultimately limits the absolute resolution of the resist. It is therefore important to be able to tailor the T_g of a resist material into a range sufficiently high to allow for effective deprotection or cross-linking while preventing diffusion induced performance degradation.

As mentioned earlier, since molecular resists generally have a well defined structure, they are well suited for the development of structure-property relation models. In an effort to better understand the glass transition behavior in these materials and to provide a predictive model to improve future resist design, a quantitative structure-property relation model based on bond additivity that allows for the prediction of the T_g of molecular resists based on their chemical structure has been developed in this work. It works well across multiple different levels of protection, different structure moieties, different molecular sizes, and different types of protecting groups.

II. MODEL DESCRIPTION

Since there is such a wide variation of molecular resist structures in literature, we classified them into several different families. Compounds are separated into families based on common structural characteristics and synthetic methods. Some of the families that we have divided molecular resists into are polyphenols, arylbenzenes, calixarenes, steroids and cholates, spirocompounds, and dendrimers. Figure 1 contains typical structures of some of these families of compounds. Polyphenols are generally synthesized by acid catalyzed condensation of phenols with ketones, aldehydes, and tertiary alcohols and usually have a triaryl carbon on which two of the aryl groups are phenols. In these cases, the triaryl carbon is generally formed by the condensation of two phenols on an aryl ketone.[20–22] Arylbenzenes are made primarily through Suzuki coupling reactions and have biphenyl type bonds linking all the aryl rings.[23] Calixarenes are cyclic compounds that are synthesized primarily through acid or base catalyzed condensation of phenols, resorcinol, pyrogallol, etc., with aldehydes which results in a cyclic compound.[24,25] Steroids and cholates are usually derived from natural products and contain a four ring carbon skeleton fashion.[26,27] Spiro compounds are characterized primarily a spiroatom that connects the molecule together.[28] The dendrimer class would include all dendrimers that are used as resists.[29] While these are not the only classes of compounds that have been used as resists, they constitute the vast majority of the designs and structures reported to date. The model developed in this article has been applied only for the polyphenol family of compounds with tert-butoxycarbonyloxy (tBoc) protecting groups and acetal type protecting groups. This family again constitutes a large portion of the molecular glass resists reported in literature by itself. Current efforts are underway to expand the current model to these other classes of compounds, and the results will be reported soon. Table I has a full list of the 57 molecular resist compounds used in developing the current model.

The primary model in this article is based on chemical bond additivity. Full molecular structures are drawn and then the compound is reduced to each of its constituent bonds. Toluene ($C_6H_5CH_3$) can be used as an example to demonstrate this method. It contains three H–C bonds (hydrogen-aliphatic carbon), one $C-C_{ar}$ bond (aliphatic carbon-aromatic carbon), six $C_{ar}-C_{ar}$ bond (aromatic carbon-aromatic carbon), and five $H-C_{ar}$ bonds (hydrogen-aromatic carbon). This is done for all the compounds studied, and the bond parameters are tabulated along with the experimental glass transition temperatures of these materials. The glass transition temperatures of the compounds are then regressed using Eq. (1) with a least squares method, where a,b,c, etc., are fitted coefficients that are the same for all compounds and N_{H-C}, $N_{H-C_{ar}}$, N_{H-O}, etc., are the number of each respective bond type for each specific molecule. Once the regression is completed on a training set of compounds, the resulting model can be used to estimate the glass transition temperature for any new polyphenol.

$$T_g = aN_{H-C} + bN_{H-C_{ar}} + cN_{H-O} + dN_{C-C} + eN_{C-C_{ar}} + \ldots . \quad (1)$$

Based on the molecular resists used for generating our model, all the compounds can essentially be broken down into 11 bond types with one correction factor needed for acetal type protecting groups. The correction factor was added because it provided a much improved fit for compounds with acetal type protecting groups and will be discussed more fully later. The correction factor used simply accounts for the total number of acetal groups on a molecule. The full list of bonds used in the model can be seen in Table II.

TABLE I. Literature molecular resists.

No.	Name	MW	Protecting group	% Protection	Expt. T_g, (°C)	Full model predicted T_g (°C)	Simplified Model Predicted T_g (°C)	Ref.
1	CR-1-0	290.36	N/A	0	58	52	52	22
2	CR-1-50	390.47	tBoc	50	42	45	45	22
3	CR-1-100	490.59	tBoc	100	33	39	38	22
4	CR-2-0	502.6	N/A	0	100	87	91	22
5	CR-2-50	702.83	tBoc	50	80	75	77	22
6	CR-2-100	903.06	tBoc	100	74	62	63	22
7	CR-3-0	714.84	N/A	0	126	123	130	22
8	CR-3-50	1015.19	tBoc	50	94	104	109	22
9	CR-3-100	1315.54	tBoc	100	83	86	88	22
10	CR-4-0	346.46	N/A	0	65	55	52	22
11	CR-4-50	446.58	tBoc	50	51	49	45	22
12	CR-5-0	620.78	N/A	0	125	105	104	22
13	CR-5-50	821.01	tBoc	50	80	93	89	22
14	CR-6-0	895.09	N/A	0	130	155	155	22
15	CR-6-50	1195.44	tBoc	50	129	136	134	22
16	CR-6-100	1495.78	tBoc	100	129	118	113	22
17	CR-7-0	424.53	N/A	0	94	71	71	22
18	CR-7-66	624.76	tBoc	66	65	59	57	22
19	CR-7-100	724.88	tBoc	100	53	52	50	22
20	CR-8-0	502.6	N/A	0	119	87	91	22
21	CR-10-0	592.72	tBoc	0	117	103	104	22
22	CR-10-50	792.95	tBoc	50	81	91	89	22
23	CR-10-100	993.19	tBoc	100	73	78	75	22
24	CR3-0	346.46	N/A	0	51	55	52	21
25	CR3-50	446.58	tBoc	50	28	49	45	21
26	CR7-0	480.64	N/A	0	56	75	71	21
27	CR5-50	506.59	tBoc	50	39	41	45	21
28	CR15-0	714.84	N/A	0	126	123	130	21
29	CRI5-tBoc-20	835.04	tBoc	20	104	114	122	21
30	CRI5-tBoc-30	895.15	t8oc	30	104	109	117	21
31	CR15-tBoc-50	1015.35	tBoc	50	94	100	109	21
32	CR15-tBoc-l00	1315.86	tBoc	100	83	76	88	21
33	CR4.0	366.45	N/A	0	67	66	64	21
34	CR4-100	566.68	tBoc	100	55	53	50	21
35	CR-9-0	578.7	N/A	0	129	102	104	21
36	CR-9-50	778.93	tBoc	50	83	89	89	21
37	CR-9-100	979.16	tBoc	100	98	77	75	21
38	CRII-0	590.71	N/A	0	107	102	104	21
39	CR11-50	790.94	tBoc	50	85	89	89	21
40	CR11-100	991.17	tBoc	100	100	77	75	21
41	CR14-100	1055.25	tBoc	100	92	91	88	21
42	CR17-0	943.13	N/A	0	165	167	168	21
43	CRI7-100	1543.83	tBoc	100	107	129	125	21
44	CR15-EE-25	823.01	Acetal EE	25	77	92	102	21
45	CR15-EE-66	1003.28	Acetal EE	66	42	41	56	21
46	CR15-CHVE-30	942.00	Acetal CHVE	30	85	92	97	21
47	CR15-CHVE-50	1093.44	Acetal CHVE	50	69	72	74	21
48	CR15-CHVE-77	1297.88	Acetal CHVE	77	49	44	44	21
49	CR15-ADE-40	1109.03	Acetal ADE	40	77	86	85	21
50	CR15-ADE-48	1187.87	Acetal ADE	48	73	79	77	21
51	CRI5-ADE-72	1424.38	Acetal ADE	72	66	57	50	21
52	3M6C-MBSA-1	981.35	N/A	0	138	129	118	20
53	3M6C-MBSA-2	1016.84	Acetal EE	8.2	106	118	109	20
54	3M6C-MBSA-3	1038.92	Acetal EE	13.5	100	112	103	20
55	3M6C-MBSA-4	1067.46	Acetal EE	19.9	109	104	96	20
56	3M6C-MBSA-5	1094.75	Acetal EE	26.2	103	96	88	20
57	3M6C-MBSA-6	1138.90	Acetal EE	36.4	91	84	77	20

TABLE II. Listing and description of bond types used in full T_g structure-property model for polyphenols.

Bond name	Description
H–C	Hydrogen-aliphatic carbon
H–C_{ar}	Hydrogen-aromatic carbon
H–O	Hydrogen-oxygen
C–C	Aliphatic carbon-aliphatic carbon
C–C_{ar}	Aliphatic carbon-aromatic carbon
C_{ar}–C_{ar}	Aromatic carbon-aromatic carbon
C_{ar}–OH	Aromatic carbon-OH
C═O–O	Carbonyl-oxygen
C_{ar}–O	Aromatic carbon-oxygen
C–O	Aliphatic carbon-oxygen
C_{ar}–C_{ar} Bi	Aromatic carbon-aromatic carbon biphenyl
Acetal	Acetal type protecting group (correction factor)

While the full set of bonds shown in Table II was created to fully describe the compounds, since all the compounds modeled were of a similar type, certain bonds types were redundant. In all the compounds studied, the H–O bonds were, in fact, all C_{ar}–OH because all the OH groups in these molecules were phenols. As a result only the C_{ar}–OH parameter was used and the coefficient for the H–O parameter was set to zero for all model fits.

While many different types of molecular representation strategies, e.g., fragment or group representations, could be used to develop the desired structure-property models, a bond model approach was chosen because a bond description can provide full characterization of a wide variety of different compounds with a relatively small number of parameters as compared to other methods such as group additivity. Bonds are also one of the simplest components of a molecule and can be more easily determined and tabulated than some fragment or group based methods. Additionally, bond additivity has shown to be effective in predicting many other important molecular properties such as heat capacity.[30]

III. RESULTS AND DISCUSSION

Before modeling the compounds, they were broken down into different classes of compounds based on their type and number of protecting groups. Unprotected compounds are the molecular resists with no protecting groups, and partially protected compounds are those with only some of their phenol units protected with protecting groups. This level of protection is expected to play an important role in determining the T_g of the compound since it affects the ability of the compound to form hydrogen bonds (e.g., fully protected compounds have all their phenol groups protected and thus are expected to lack significant hydrogen bonding effects). While most of the molecular resists in literature have tBoc protecting groups, there are also some reported with acetal type protecting groups with the most common form being 1-ethyl-1-ethoxy ethers made from ethyl vinyl ether.

Table III lists the best fit coefficients for all unprotected, partially, and fully tBoc protected compounds, along with the coefficients for all the acetal type protecting groups. The coefficient of determination (R^2) and the 1σ standard deviation between the experimental and predicted T_g values are listed in Table III as well. Since there are significantly fewer compounds in literature with acetal type protecting groups, they were not broken down into partially and fully protected compounds. No acetal correction term was included in the acetal class because all the contributions of the C_{ar}–O and C–O bonds came from acetal groups and so the acetal correction factor is redundant in this class. Comparing the R^2 values for the four different classes of compounds, the model does a good job of correlating the T_g of the various compounds in all cases. The partial tBoc protected and acetal protected compounds can be especially well predicted by the model with R^2 values of 0.93 or greater and a standard deviation of 7.05 °C or less, but they have more parameters than the unprotected and fully tBoc protected compounds and so these extra degrees of freedom could also be partially responsible for the better quality of the model fits.

TABLE III. Best fit coefficients for all unprotected, partially, fully tBOC protected polyphend compounds and compounds with acetal protecting groups.

	tBoc protection level			
Bond name	None	Partial	Full	Acetal protected
H–C	15.42	0.50	0.05	0.24
H–C_{ar}	6.18	−0.61	1.15	1.00
H–O				
C–C	−42.22	−2.20	−0.65	0.60
C–C_{ar}	−16.18	0.95	6.63	2.20
C_{ar}–C_{ar}	−0.11	2.48	0.69	0.28
C_{ar}–OH	17.63	2.56		5.65
C═O–O		1.08	−0.63	
C_{ar}–O		−0.97	−1.95	−1.10
C–C		0.98	0.09	−3.55
C_{ar}–C_{ar} Bi	−9.74	−9.16	2.44	
Acetal				
Statistics				
R^2	0.85	0.94	0.83	0.93
σ	12.92	6.62	10.87	7.05

Comparing the values for the various parameters across different classes in Table III, some interesting trends appear. For all compounds, the C_{ar}–OH parameter shows a strong influence on increasing T_g in all compounds. This is expected due to the strength of hydrogen bonding and the influence such hydrogen bonding can have on molecular motion. In the unprotected compounds, C_{ar}–OH bonds show the strongest effect on increasing T_g, while the C–C bond has the strongest effect on decreasing T_g due to the flexibility of this type of bond. In unprotected and partially tBoc protected compounds, the C_{ar}–C_{ar} biphenyl bond has a negative effect on T_g, while in the fully protected compounds, it acts to increase T_g. This is unexpected given the relative stiffness of a biphenyl bond, but it may act to hinder molecular movement enough to reduce the effect of hydrogen bonding in unprotected and partially compounds, while this hindrance acts to

TABLE IV. Best fit coefficients for the full bond model and simplified model for all compounds.

Bond name	Model coefficient	
	Full	Simplified
H–C	0.36	
H–C_{ar}	1.18	
H–O	0.00	
C–C	0.23	
C–C_{ar}	0.85	
C_{ar}–C_{ar}	1.46	2.08
C_{ar}–OH	3.09	7.14
C═O–O	−1.77	
C_{ar}–C	−3.28	
C–C	−0.35	
C_{ar}–C_{ar} Bi	0.95	
Acetal	−16.90	−11.55
Statistics		
R^2	0.84	0.81
σ	12.02	13.12

increase the T_g in fully protected compounds because it reduces molecular movement but no longer negatively affects the ability of molecules to form hydrogen bonds. Across all compounds, protecting the phenols acts to decrease T_g by reducing the hydrogen bonding as indicated by the positive value for C_{ar}–OH bonds and increasing flexibility at the point where the protecting group attaches to the molecule as indicated by the C_{ar}–O bond parameter.

While the model may work well for each individual class of compounds, it is more useful if it can predict T_g across all of the classes of polyphenols. Table IV shows the full model fit for all the molecular glass compounds in this study, along with a simplified model that will be discussed later. A comparison between the predicted and experimental T_g values is seen in Fig. 2. The model works well across all compounds with an R^2 value of 0.84 and a standard deviation of 12.02 °C. The coefficients produced from the fit of the model across all compounds provide insight into the major

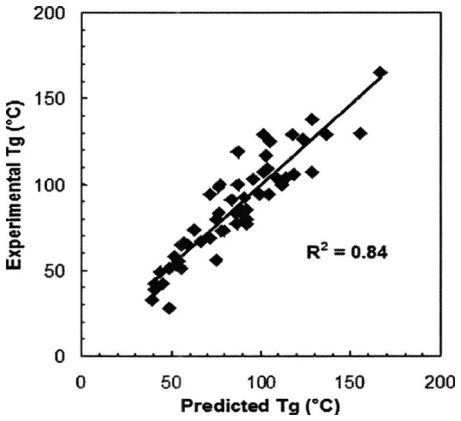

FIG. 2. Comparison between the experimental values and full bond model predicted values of T_g.

factors that affect T_g behavior in these materials. The two dominant factors in increasing T_g are C_{ar}–OH bonds and C_{ar}–C_{ar} bonds. Increasing C_{ar}–OH bonds increases T_g due to increased hydrogen bonding. C_{ar}–C_{ar} bonds are present in the aromatic rings which are stiff relative to many other bonds and thus increase T_g. The same argument applies to C_{ar}–C_{ar} biphenyl bonds which show a relatively large positive coefficient. The major factors in decreasing T_g are all associated with addition of protecting groups to the molecules, with the C═O–O, C_{ar}–O, and C–O bonds that are important being found in the tBoc groups. Introducing the more flexible esters and ether linkages into the molecules acts to decrease the T_g. The acetal correction factor has a large negative value indicating that there is a large penalty to T_g associated with the introduction of acetal protecting groups. This is likely due to the highly flexible nature of the acetal bond.

Despite the fact that reasonably good fits could be obtained for all the compounds using the full bond model, the fundamental factors affecting T_g are better found by carrying out a principal component analysis of the parameters in the model. While a principal component analysis can be carried out through many different methods,[31] the principal component analysis in this case was done by setting one coefficient at a time to zero, performing a nonlinear least squares regression on the model without this parameter, and comparing the R^2 value for the model with and without this parameter. In this manner, one parameter at a time was removed from the model until the minimum number of parameters required to obtain a good fit was obtained. It was found that all the polyphenol compounds studied in this work could be well fitted using only three parameters: C_{ar}–OH, C_{ar}–C_{ar}, and the acetal correction factor. The full model and the simplified model parameters along with the R^2 and standard deviations between each model predicted T_g and experimental T_g are listed in Table IV. The reduced model still gives a very good fit for all compounds with only a slightly smaller R^2 value of 0.81 and a slightly larger standard deviation of 13.12 °C than the full bond model.

Since all the C_{ar}–C_{ar} bonds in these compounds are found only in the aromatic rings (ArRings), the best fit simplified model can be succinctly written in Eq. (2). Since there are six C_{ar}–C_{ar} bonds in a ring, the ArRings coefficient is just the C_{ar}–C_{ar} coefficient from the simplified model multiplied by six. Equation (2) provides insight into the T_g behavior of these systems. This simplified model works well for the compounds studied in this article because they all are polyphenols and have very similar structural elements. The aromatic ring parameter implies that when the number of aromatic rings in a molecule is increased, more concerted motion is required to cross the glass transition. Since the rings are relatively stiff compared to other bonds, increasing the number of aromatic rings increases the T_g. While increasing the number of aromatic rings acts to increase the molecular weight, the ring factor is more than just a molecular weight effect. If a model is used that is based on molecular weight, C_{ar}–OH bonds, and acetal groups instead of the current model, a sig-

nificantly worse fit to the experimental data is obtained compared to the model described in Eq. (2). As described before, the effect of C_{ar}–OH groups is to increase the T_g of the material by increased hydrogen bonding between molecules, and acetal groups act to decrease the T_g by increasing the flexibility of the molecule.

$$T_g = 7.138N_{C_{ar}\text{–OH}} + 12.500N_{\text{ArRings}} - 11.547N_{\text{acetal}}. \quad (2)$$

While addition of tBoc protecting groups acts to decrease the T_g by reducing the number of C_{ar}–OH groups, no additional factor for tBoc groups is required in the simplified model. The larger coefficient for the C_{ar}–OH parameter compared to the full bond model accounts for the T_g penalty of tBoc protection. This is not the case for acetal protecting groups. An additional penalty beyond loss of C_{ar}–OH bonds must be added to the model through the acetal correction factor to properly reflect the influence of acetal group addition on T_g. If no acetal factor is included in the simplified model, the R^2 value is reduced to 0.62 and the standard deviation increases to 18.57.

IV. CONCLUSIONS

A bond contribution model has been developed for the prediction of glass transition temperatures in polyphenol molecular glass resists. It does a good job of predicting T_g with a R^2 of 0.84 compared to experimental T_g values and a standard deviation of only 12 °C. T_g is found to increase as the number of C_{ar}–OH bonds in the molecule increases due to the increased ability of the molecule to form hydrogen bonds. Stiff structural moleties such as aromatic rings and biphenyl bonds also acts to increase T_g by reducing the flexibility of the molecule. Adding protecting groups tends to decrease T_g due to reduced hydrogen bonding and increased flexibility of the protecting group linkages. Acetal type protecting groups have an even stronger effect than tBoc protecting groups on decreasing T_g due to the higher flexibility of the acetal group compared to the carbonate group. The model was also simplified to a three parameter model that predicts the T_g of molecular glass resists nearly as well as the full bond model. The simplified model provides a good and fast heuristic for molecular resist design.

ACKNOWLEDGMENTS

The authors would like to gratefully acknowledge Intel Corporation for funding this research and would also like to thank Dr. Jeanette Roberts, Dr. Steve Putna, Dr. Todd Younkin, and Dr. Wang Yueh at Intel for helpful discussions related to this work. The authors would also like to acknowledge Professor Laren M. Tolbert and Professor Peter Ludovice at Georgia Tech for helpful discussion related to this work.

[1] Y. Shirota, J. Mater. Chem. **10**, 1 (2000).
[2] T. Hirayama, D. Shiono, H. Hada, J. Onodera, and M. Ueda, J. Photopolym. Sci. Technol. **17**, 435 (2004).
[3] J. Y. Dai, S. W. Chang, A. Hamad, D. Yang, N. Felix, and C. K. Ober, Chem. Mater. **18**, 3404 (2006).
[4] D. Yang, S. W. Chang, and C. K. Ober, J. Mater. Chem. **16**, 1693 (2006).
[5] D. Shiono, H. Hada, H. Yukawa, H. Oizumi, I. Nishiyama, K. Kojima, and H. Fukuda, Proc. SPIE **6519**, 65193U/65191 (2007).
[6] R. A. Lawson, C.-T. Lee, L. M. Tolbert, and C. L. Henderson, Microelectron. Eng. **86**, 738 (2009).
[7] R. A. Lawson, C.-T. Lee, W. Yueh, L. Tolbert, and C. L. Henderson, Proc. SPIE **6923**, 69230K/1 (2008).
[8] F. Ashrafi, A. A. Rostami, and N. M. Pour, Asian J. Chem. **21**, 1667 (2009).
[9] Q. Wang, P. S. Ma, C. Wang, and S. Q. Xia, Chin. J. Chem. Eng. **17**, 254 (2009).
[10] B. Moller, J. Rarey, and D. Ramjugernath, J. Mol. Liq. **143**, 52 (2008).
[11] Y. Nannoolal, J. Rarey, and D. Ramjugernath, Fluid Phase Equilib. **269**, 117 (2008).
[12] D. Sola, A. Ferri, M. Banchero, L. Manna, and S. Sicardi, Fluid Phase Equilib. **263**, 33 (2008).
[13] A. R. Katritzky, I. B. Stoyanova-Slavova, D. A. Dobchev, and M. Karelson, J. Mol. Graphics Modell. **26**, 529 (2007).
[14] S. H. Hilal, A. N. Saravanaraj, T. Whiteside, and L. A. Carreira, J. Comput.-Aided Mol. Des. **21**, 693 (2007).
[15] H. Ito, Adv. Polym. Sci. **172**, 37 (2005).
[16] D. S. Fryer, S. Bollepali, J. J. de Pablo, and P. F. Nealey, J. Vac. Sci. Technol. B **17**, 3351 (1999).
[17] T. Fujigaya, Y. Shibasaki, and M. Ueda, J. Photopolym. Sci. Technol. **14**, 275 (2001).
[18] M. D. Stewart, S. V. Postnikov, H.-V. Tran, D. R. Medeiros, M. A. Nierode, T. Cao, J. Byers, S. E. Webber, and C. G. Willson, Polym. Mater. Sci. Eng. **81**, 58 (1999).
[19] M. D. Stewart, H. V. Tran, G. M. Schmid, T. B. Stachowiak, D. J. Becker, and C. G. Willson, J. Vac. Sci. Technol. B **20**, 2946 (2002).
[20] T. Hirayama *et al.*, Proc. SPIE **5753**, 738 (2005).
[21] A. De Silva, N. Felix, J. Sha, J.-K. Lee, and C. K. Ober, Proc. SPIE **6923**, 69231L/69231 (2008).
[22] A. De Silva, J. K. Lee, X. Andre, N. M. Felix, H. B. Cao, H. Deng, and C. K. Ober, Chem. Mater. **20**, 1606 (2008).
[23] A. De Silva and C. K. Ober, J. Mater. Chem. **18**, 1903 (2008).
[24] H. Ito, T. Nakayama, M. Sherwood, D. Miller, and M. Ueda, Chem. Mater. **20**, 341 (2008).
[25] K. Young-Gil, J. B. Kim, T. Fujigaya, Y. Shibasaki, and M. Ueda, J. Mater. Chem. **12**, 53 (2002).
[26] D. Shiono, T. Hirayama, H. Hada, J. Onodera, T. Arai, A. Yamaguchi, K. Kojima, H. Shiraishi, and H. Fukuda, Proc. SPIE **6153**, 61532D/61531 (2006).
[27] D. Shiono, T. Hirayama, K. Kasai, H. Hada, J. Onodera, T. Arai, A. Yamaguchi, K. Kojima, H. Shiraishi, and H. Fukuda, Jpn. J. Appl. Phys., Part 1 **45**, 5435 (2006).
[28] F. Pfeiffer, N. M. Felix, C. Neuber, C. K. Ober, and H. W. Schmidt, Phys. Chem. Chem. Phys. **10**, 1257 (2008).
[29] D. C. Tully, A. R. Trimble, and J. M. J. Frechet, Adv. Mater. (Weinheim, Ger.) **12**, 1118 (2000).
[30] H. E. O'Neal and M. A. Ring, Inorg. Chem. **5**, 435 (1966).
[31] I. T. Jolliffe, *Principal Component Analysis*, 2nd ed. (Springer, New York, 2002).